The analysis of H/V curve from different ellipticity retrieval technique for a single 3c-station recording.

1. Irfan Ullah : Corresponding Author
Email: syed_528@yahoo.com
Telephone : +5511 3091-2789
Fax: +5511 3091-5034
Adress: Department of Geophysics - IAG Sao Paulo University - USP Rua does Matão, 1226, Cidade Universitária CEP-05508-090 - Sao Paulo, Brasil.

2. Renato L.PRADO **:** Department of Geophysics - IAG Sao Paulo University - USP Rua does Matão, 1226, Cidade Universitária CEP-05508-090 - Sao Paulo, Brasil.

Abstract.

In the last two decades or so the H/V (Horizontal-to-Vertical Spectral Ratio) technique remained very popular, and are extensively used for the site fundamental frequency estimation. H/V curve is also used with dispersion curve to jointly invert and retrieved the shear wave velocity of relatively deep soil deposit. Although a full theoretical explanation of H/V technique is not been presented yet, there are two main assumptions used generally that H/V curves can be explained by considering Rayleigh wave of noise wave field only while the other newly presented approach utilizes the whole noise wave field known as diffuse field approach (DFA). However in case of Rayleigh wave approach for H/V, it is almost impossible to the remove the fraction of Love wave from the horizontal component of H/V. Here in this study we aim to test different approaches adopted for the removal of Love wave fraction from horizontal component for a borehole test site at University of Sao Paulo. The result from different approaches are compared with borehole ellipticity curve. It is concluded that around the fundamental frequency the H/V obtained in either way(DFA or ellipticity approach) is dominated by Rayleigh waves.

1. Introduction.

H/V (Horizontal-to-Vertical spectral ratio) is fast and quick way to get properties of a site for engineering interest, by the measurement of ambient noise wave field with a single 3-component sensor on the earth surface. The method is used for rapid estimation of fundamental resonance frequency (f_0) of a site where the maximum displacement amplification is expected in case of an earthquake. This technique is also used to retrieve the shear wave velocity of the geological structure in a joint inversion with dispersion curve (Scherbaum et al, 2003 Picozi et al, 2005 Hobiger et al, 2013). However, some controversies about the nature of ambient noise wave field and sources exist, which most of the time make the results of H/V curve questionable and hence debatable. Apart from the controversies exist in nature of ambient noise wave filed M. Mucciarelli et al (2001) described some problem regarding the acquisition and processing of H/V spectral ratio. Due to extensive utilization of H/V technique, a commission was established to test the acquisition, processing and interpretation of this technique (site effects assessment using ambient excitations) – the SESAME project (2001-2004), The guidelines reports are published for acquisition, processing and interpretation of ambient noise wave field and have addressed all the points raised and discussed by M. Mucciarelli et al (2001) in extensive details. The H/V curve is modeled with different approaches and each modeling approach might have the effect on

the retrieved soil profile(Sanchez-Sesma et al, 2011, Lunedei & Malischewsky 2015). The acquisition of the data is made with a three component sensor placed on the surface of ground which record the seismic noise wave field. Fourier spectra of the recorded seismic noise for all the three component (eat-west , north-south and vertical) are calculated. The two horizontal component Fourier spectra are properly averaged and then divided by the vertical Fourier spectra. This division of averaged horizontal and vertical component result a curve (H/V) as function of frequency. H/V curve usually result a peak depending on the subsoil stratigraphical profile, this peak correspond to fundamental resonance frequency (f_0) of the site (Tokimatsu, 1997; Bard, 1999; Bonnefoy-Claudet et al., 2006). The averaged horizontal component of H/V curve contains the contribution from both Rayleigh and Love wave and some fraction of body waves as well. In a joint inversion of H/V curve with dispersion curve this other elastic wave effect presence in the H/V curve might bias the retrieved s-wave velocity profile. Therefore, the presence of Love and other elastic waves existence in the H/V curve must be assumed or estimated before the inversion process (Bonnefoy-Claudet et al., 2006). Here in this communication we will try to list the different approaches used for refining of the H/V curve by removing unwanted fraction (Love wave effect presence) prior to the joint inversion with dispersion curve. At present there are two main research lines describing the H/V curve by taking in account the whole ambient-vibration wave field, and another just studies the surface wave and Rayleigh wave dominancy in noise wave field (Lunedei & Malischewsky 2015). Sanchez-Sesmaet al (2011) proposed that seismic noise field can be consider as diffusion-like situation which contain all type of elastic wave (surface and body waves) . He suggested that the average autocorrelation of the motions at a given receiver, in the frequency domain, measures the directional energy density (DED) and is proportional to the imaginary part of the Green function (GF) when both source and receiver are the same. The surface wave dominancy opinion of noise wave field is in favor of Rayleigh wave dominancy (Yamamoto, 2000 Boremann 2002, Cornou, 2002 , Okada ,2003). We will try to check both these assumptions here with the borehole data.

The site for which this analysis are made is a borehole site at university of Sao Paulo shown in Fig.1. The noise measurement were made with broadband 3 component seismometer nanometrics Trillium Compact 120-s. Ambient noise wave field measurements were made for 24 hours on weekend night to minimized cultural noise influence. The data acquisition of ambient noise has been done following the guidelines developed under the SESAME (2004) recommendations. To obtain the fundamental frequency of the site a window of one-hour recording were processed and the reliability condition proposed by SESAME (2004) for the H/V curve and peak were followed.

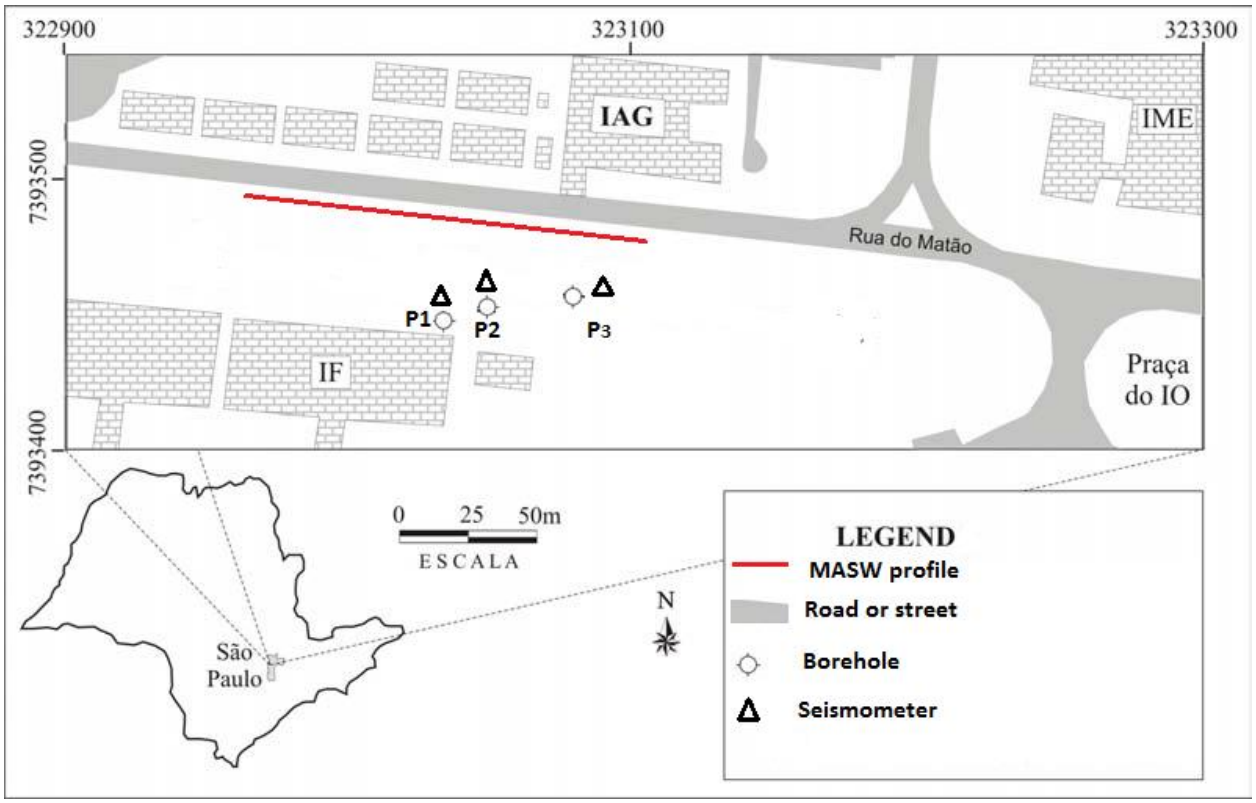

Fig. 1 shows the location map studied area ,legends explain the different symbols. (modified from Porsani 2004).

We will try to discuss briefly here and analyzed our seismic noise data with this diffuse-field assumption (DFA). Later we will analyzed our data with assumption that H/V curve basically reflect the Rayleigh wave ellipticity.

2. Diffuse field assumption technique.

Sanchez-Sesma et al (2011) proposed to considered ambient noise wave field as diffuse wave field which contain all different types of waves (surface and body). The ambient noise wave field is generated by multiple random uncorrelated forces/sources near to or at the earth surface. The wave field may contain the scattering effect of various elastic mode. The field intensities could be in a better way described by diffuse like situation. To assume that the noise wave field is diffuse, the H/V curve can be estimated for a receiver at earth surface in term of green tensor imaginary part at the source (source and receiver are assumed to be at same location). The work of Sanchez-Sesma provides an idea of linkage between energy density and imaginary part of GF in 3D (energy densities of the noise wave field is proportional to the imaginary part of green tensor). The H/V curve obtained from the square root ratio of imaginary parts of GF (horizontal and vertical components) Eq.2 serve as intrinsic property of medium therefore its inversion can be used to retrieved subsurface soil profile. The detailed analysis of the method is beyond the scope of this article, interested readers are referred to Sanchez-Sesmaet al (2011) for more detail. The summary of this procedure is that autocorrelation of motion at a receiver sensor in a given direction is proportional to directional energy density (DED),and this DED is proportional to the imaginary part of Green tensor at that sensor (Sanchez-Sesmaet al 2011).

Patron et al. (2009) showed that in case of 3D homogeneous elastic half space, the horizontal displacement (radial and transverse) have fix energy proportion (e.g $E_1(x,x,\omega) = E_2(x,x,\omega)\ and\ also\ ImG_{11}(x,x,\omega) = ImG_{22}(x,x,\omega)$).For a diffused wave field the H/V can be represented in term of directional energy densities assuming source and receiver lies at same location (x) on the surface of earth as

$$\frac{H}{V}(\omega) = \sqrt{\left(\frac{E_1(x,x,\omega)+E_2(x,x,\omega)}{E_3(x,x,\omega)}\right)} \quad (1)$$

$$\frac{H}{V}(\omega) = \sqrt{\left(\frac{ImG_{11}(x,x,\omega)+ImG_{22}(x,x,\omega)}{ImG_{33}(x,x,\omega)}\right)} \quad (2)$$

where in (1)

$E_m(x,\omega) = \rho\omega^2\langle u_m(x,\omega)u_m{}^*(x,\omega\rangle \quad$ where m = 1,2,3

$= -2\pi\mu E_s k_s{}^{-1} Im[G_{mm}(x,x,\omega)]$

$E_1(x,x,\omega), E_2(x,x,\omega)$ and $E_3(x,x,\omega)$ are the energy density at coincident source and receiver (x,x) at frequency ω and subscript 1,2 show both the horizontal (east-west, and north south) while 3, that of vertical component. Energy density is find out at point x in direction m. $\omega, \rho\ and\ u_m$ are angular frequency , layer density and displacement at point x respectively . $E_s = \rho\omega^2 s^2$ is the strength of diffuse illumination in term of shear wave average energy density μ is shear wave modulus $\langle \ldots \rangle$ bracket shows the azimuthal average, k_s=$\frac{\omega}{V_s}$ shear wave number V_s shows medium S-wave velocity. The symbol (.*) show complex conjugate process, the medium response in a direction m (of impulse load and acting in same direction) is indicated by G_{mm} .The H/V curve obtained in this manner is linked to the intrinsic property of medium , The resulted H/V curve from the diffuse-field approach might allow its inversion without considering any supplemented information (dispersion curve).

For our analysis, the data of seismic noise recorded at borehole test site were analyzed with DFA (diffuse field assumption) frame work of Eq.2 , $\frac{H}{V}(\omega)$ results are obtained from 50 windows each of length 50 seconds, each window is normalized as suggested by Jose Pina Plores et al (2016) .The curve obtained by this directional energy density approach is compared with borehole ellipticity Fig.2. The peak and trough of H/V curve obtained (Fig.2) correspond to peak and trough of ellipticity. However the shape of H/V curve is generally higher except the peak ,it is because of other elastic wave phases contribution. This peak and trough correlation of the H/V curve with borehole ellipticity might shows that at these singularities (peak and trough) Rayleigh wave ellipticity dominate the shape of H/V. It is important to note here the inversion of ellipticity curve with dispersion curve are recommended around the peak and right limb of the H/V curve (Picozi et al. 2005 Hobiger et al. 2013). It is to be noted that all this H/V computation in this case is resting on the assumption that noise wave field is diffused. Is it?. Mulagia (2012) statistically check this assumptions of diffused field for noise at 65 different locations for diverse geological conditions and recording environment. He showed statistically that the seismic noise wave field is not diffused as the noise wave field is not azimuthally isotropic. In the next section we will focus our attention on the other line of research which is in the opinion of, that noise wave field is dominated by surface wave especially Rayleigh wave (see section 3) , and H/V curve can be explained by its correlation with Rayleigh wave ellipticity curve (Bard 1999).

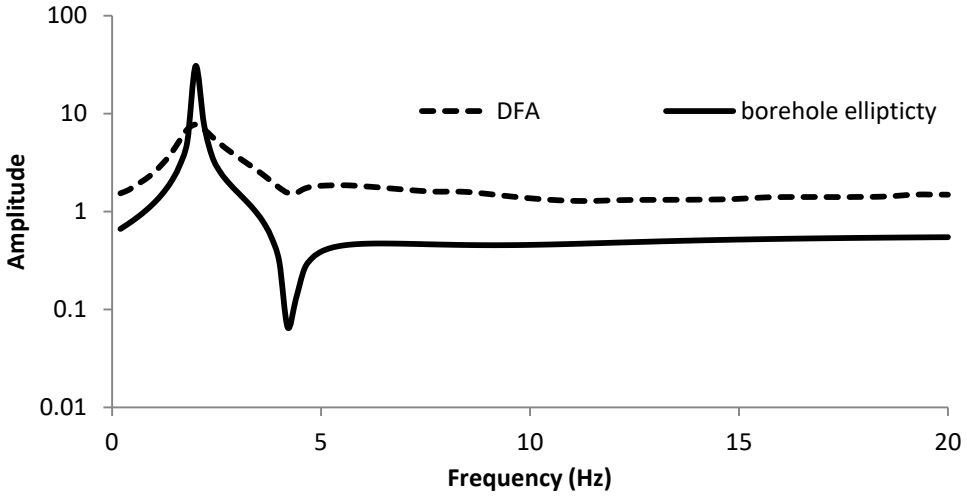

Fig.2 H/V curve obtained through DFA technique at the test site (IAG-USP), the Borehole ellipticity curve is plotted in solid for comparison at the site.

3. Surface wave dominancy of noise wave field.

To find out that whether body or surface waves dominate the full wave field, is analyzed by Bormann (2002) , He used sensors for earthquake and seismic noise recording both at the surface and in the boreholes at different depth levels and concluded the surface-wave nature of seismic noise Fig. 3. Bormann (2002) showed that, the penetration depth of surface waves increases with wavelength, high frequency noise attenuates more rapidly with depth. In case of Fig.3 the noise power at 300 m depth in a borehole was reduced, as compared to the surface, by about 10 dB, at f = 0.5 Hz, 20 dB at 1 Hz and 35 dB at 10 Hz. This continuous amplitude decline with frequency is in accord with the surface waves nature of seismic noise.

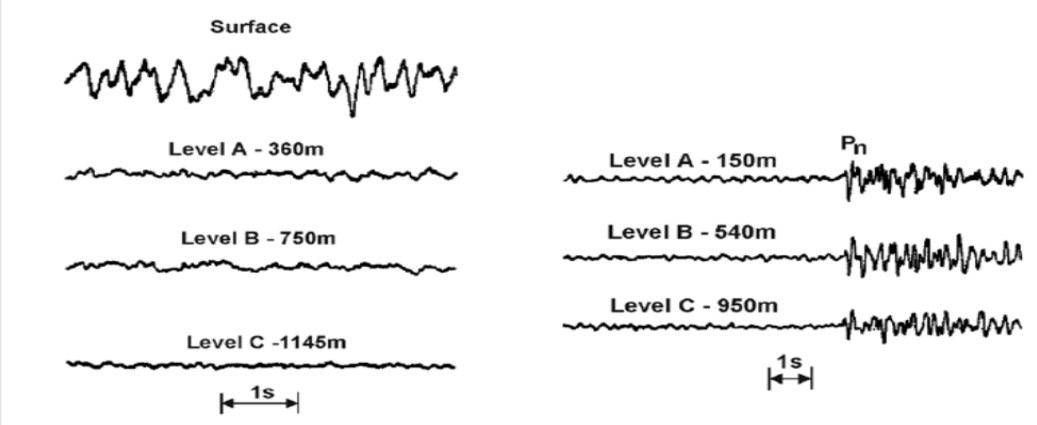

Fig.3.Recording of seismic noise (left) and earthquake signals (right) at the surface and at different depth levels of a borehole. (Bormann 2002).

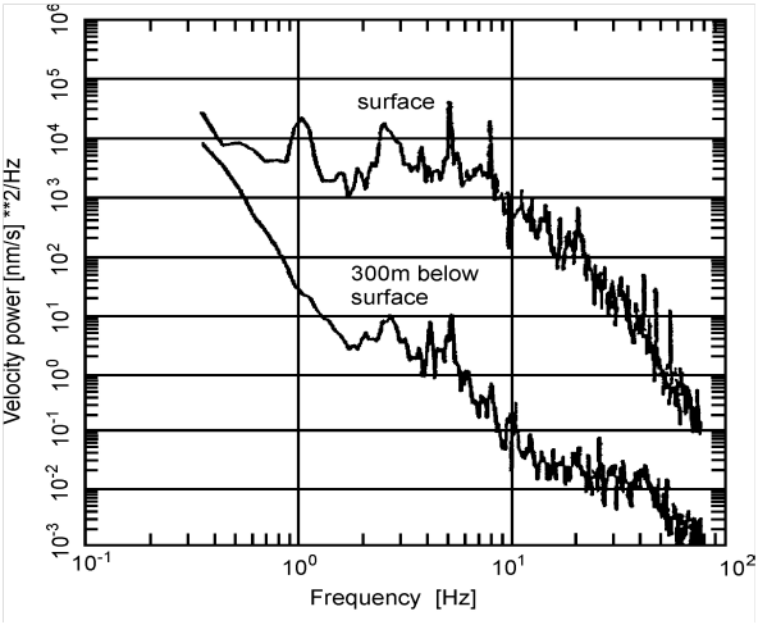

Fig. 4 Velocity power density spectra as obtained for noise records at the surface (top) and at 300 m depth in a borehole (below) near Gorleben, Germany (Bormann , 2002).

If the noise wave field is mainly dominated by surface wave then another question arises , that what is the fraction of contribution of Rayleigh and Love waves to the full noise wave field. Most of the researchers focused their attention to find the fraction Rayleigh to Love ratio from the analysis of noise wave field recorded on vertical component (Li et al., 1984; Horike, 1985; Yamanaka et al., 1994). The results of these studies showed an agreement in one aspect that microseism (<1Hz) are mainly dominated by Rayleigh waves however at high frequency (> 1Hz) a combination of P and Rayleigh wave exists .Table 1 summarize the result of previous studies on this issue.

	Rayleigh waves	**Love waves**	**frequency range**
Chouet et al.,1998	**30%**	**70%**	**>2Hz**
Yamamoto, 2000	**<50%**	**>50%**	**3-10 Hz**
Arai et al., 1998	**30%**	**70%**	**1-12 Hz**
Cornou, 2002	**60%**	**40%**	**< 1 Hz**
Okada (2003)	**<50%**	**>=50%**	**0.4-1 HZ**

Köhler(2006)	**10–35%**	**65–90%**	**0.5–1.3 Hz**

Table 2 Summary conclusions about the proportion of Rayleigh and Love waves in noise.

4.Removal of Love wave from horizontal component.

Rayleigh waves are formed by the linear pairing of P (primary waves) and Sv (vertically polarized shear waves) waves (Aki, 2002).This pairing of vertical and horizontal components have a phase shift of $\pm\frac{\pi}{2}$, the particle motion induced by Rayleigh waves will dipict an ellipse. This elliptical motion will either be retrograde or prograde depending on the sign of phase shift. Similarly Love wave is composed of horizontally polarized shear waves (SH). The horizontal over vertical axes of ellipse described by particle motion under the Rayleigh wave influence is termed as ellipticity. At situation of homogeneous half-space the particle motion is retrograde at all frequencies and ellipticity is constant . However in case of layered structure ellipticity exhibit a peak and trough and the particle motion switch from retrograde to prograde and then to retrograde with the frequency, depending on the velocity contrast between the soil and bedrock (Konno and Ohmachi, 1998).

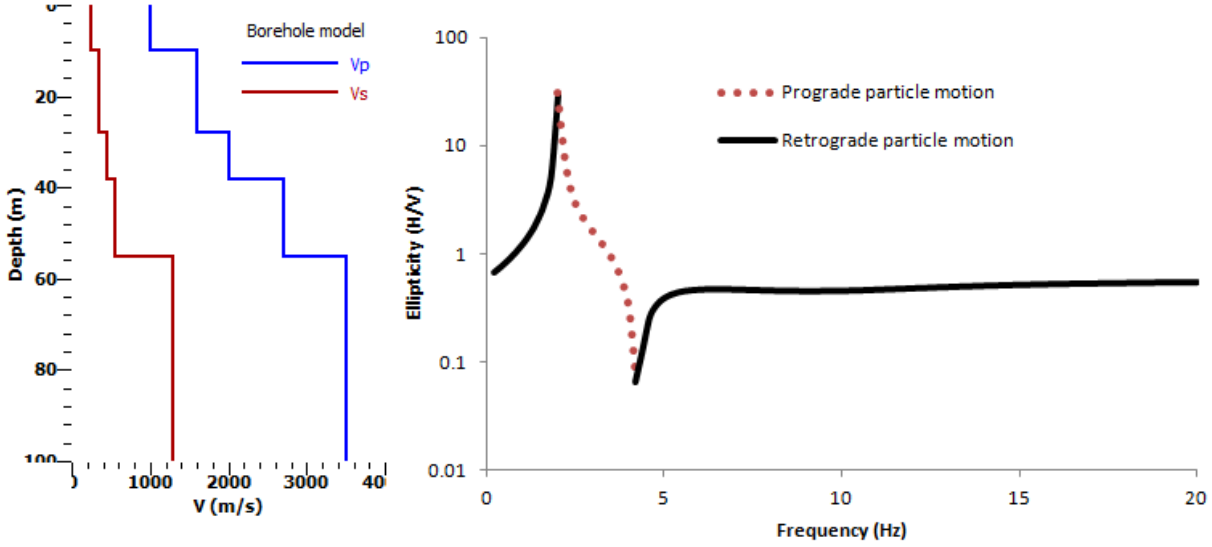

Fig.5 Borehole model at IAG-USP . The ellipticty curve of fundamental Rayleigh wave of the borehole model , marking the frequency ranges where the retrograde and prograde motion might occur.

The conclusion from the preceding section can be drawn that, the contribution of Love wave to the horizontal is not predictable and fluctuate with frequency and from site to site. The H/V spectral ratio are linked to the ellipticity of Rayleigh wave , in situation where the high shear

wave contrast exist between soil and bedrock (Bard,1999).The H/V curve corresponds nicely to the peak of ellipticity curve (Fig.5). The deviation between curves can be easily linked to the presence of Love wave contribution to noise wave field at the horizontal component. We will try to review all the available technique for the this task and compared its result with borehole ellipticity.

H/V curves are obtained and compared with the elliptiity curve of borehole at the same site. The deviation between the curves are due to Love wave contribution. H/V curve is generally higher than the ellipticity curve except at peak frequency of Rayleigh wave ellipticity Fig.6. Three different polarization techniques are used to minimized the effect of Love wave. The first technique is the simple H/V of seismic noise (Fig.5) , In this technique the polarization mean the division of Fourier spectral amplitude of averaged horizontal component over vertical component with the assumption that around the fundamental resonance frequency the vertical component is dominated by Rayleigh only. Generally it is believed that Rayleigh (P-SV) and Love wave (SH) contribute equally to the horizontal component. Fäh et al (2001) proposed the division of H/V spectral amplitude by $\sqrt{2}$ for Love wave effect minimization from horizontal component Fig.5. However this is not a wise approach because the energy partition of horizontal component between Rayleigh and Love is not constant and varies with frequency and site (Köhler *et al.* 2006; Endrun 2011) see also Table 1. There are two other polarization approaches employed for this job recently are: time-frequency analysis (Fah et,al 2009) and RayDec (Hobiger et, al, 2009).

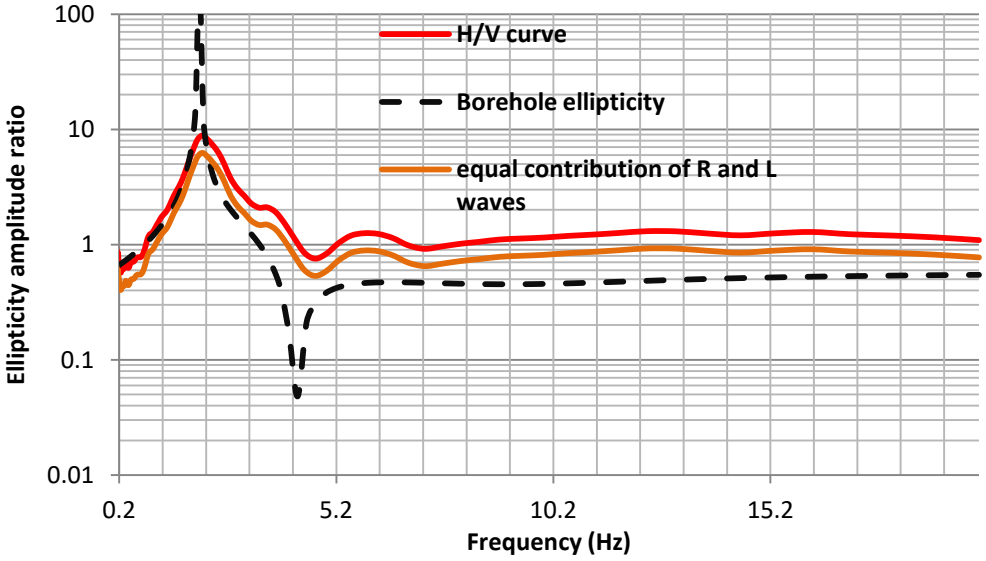

Fig.6 shows the comparison of H/V curve of experimental data recorded at test borehole site at university of Sao Paulo.

5. Time-frequency analysis.

In time-frequency analysis the vertical component of noise wave field is considered as a trigger and its energy level are estimated at given time and frequency and correlated with horizontal components (east-west , and north- south). A brief description of the technique is that continuous wavelet transformation (CWT) are performed on the east e(t) , north n(t) and vertical v(t) components of noise wave field. CWT (continuous wavelet transform) transform a signal to time-scale plane. The scale is a single parameter which controls both the duration and bandwidth.CWT is defined as:

$$\mathrm{CWT}_{x(t)}(a,b) = \frac{1}{\sqrt{a}}\int_{-\infty}^{\infty} x(t)\psi^{*}\left(\frac{t-b}{a}\right)dt \qquad (3)$$

where x(t) is real-valued signal component {where $x(t) = e(t)$ or $n(t)$ or $v(t)$ }, *ψ(t)* shows the mother wavelet,* shows a complex conjugation process, a scale parameter (scale control both the duration and bandwidth) b is translation in time. Fah et,al (2009) used a modified Morelet wavelet in a code written for this job due the reason that traditional Morelet wavelet does not work satisfactorily for H/V analysis. The modified Morelet transform is defined as

$$\psi(t) = \exp(i2\pi ft)e^{\left(\frac{-t^2}{m}\right)} \qquad (4)$$

here f is the central frequency of the wavelet, m control the resolution of both frequency and time, low m mean more time resolution on the expense of low frequency localization and higher m result on the contrary i.e increase frequency resolution at the expense of low time localization. The classical Morelet wavelet is achieved when m=1/2. After the application of CWT to each component of a single 3-c sensor recording $\{e(t), n(t) \text{ or } v(t)\}$ give rise to three signals amplitude which is both the function of time and frequency. Two horizontal $(e(t), n(t))$ component are merged together to a single component. As Rayleigh wave are the result of the coupling of P-waves and vertically polarized S-waves, the vertical component is sorted out for amplitude maxima at each frequency and time translation . Similarly, the horizontal component is analyzed for amplitude maximum at given frequency and time, the horizontal components are phase shifted $\pm$ at a quarter of the period. This shift of period is done because of theoretical phase shift between $\pm\frac{\pi}{2}$ vertical and horizontal component particle motion. For each maximum on the vertical component, the corresponding maximum on the horizontal component are stored and the ratio of H/V are estimated. The effect on the length of the recorded signal is shown in Fig.7. There is only one tuning parameter m ,the effect of its different values are shown in Fig.8. This whole process is statistically analyzed by histogram for all the frequency and translation of time and H/V is obtained by the maximum of each histogram. For detail theoretical outline of this analysis please read (Fah et,al, 2009).

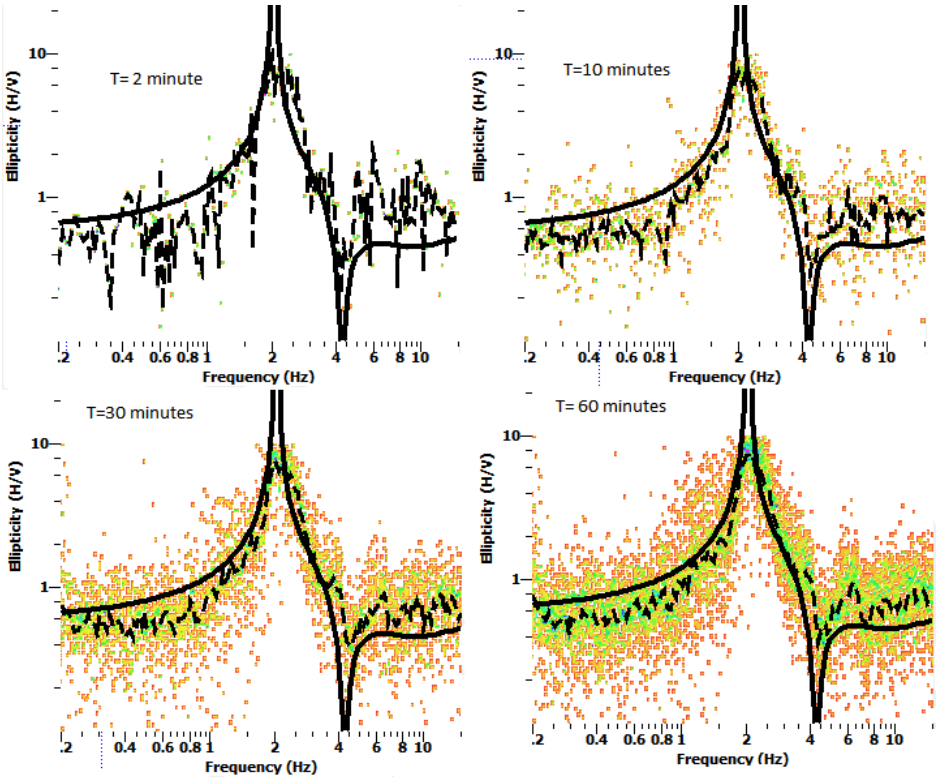

Fig.7 Ellipticity (H/V) obtained from continuous wavelet transformation CWT for diffrent length of the recorded signal; a histogram is drawn for each frequency, the color within histogram indicates the energy level. (dashed line shows ellipticity obtained from CWT while solid line shows the ellipticity curve obtained from borehole data at same location - IAG-front)

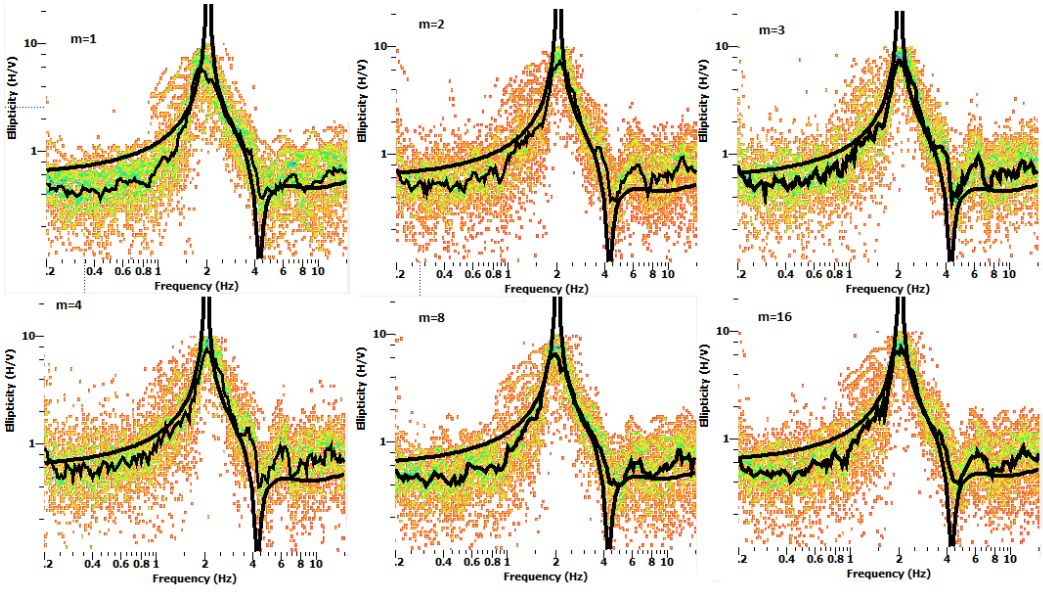

Fig.8 Ellipticity (H/V) obtained from continuous wavelet transformation CWT for diffrent value of m; (curvy line shows ellipticity obtained from CWT while solid line shows the ellipticity curve obtained from borehole data at same location - IAG-front)

Fig.7 and 8 show a better result when compared with the borehole ellipticity curve of borehole. The result of wavelet transform Fig.6&7 shows that the ellipticity of borehole is retrieved in better way(especially at right limb of the ellipticity) when the recorded length of the signal is greater than 30 minute ,and when the value of $m \geq 8$.

6 Random decrement technique (RayDec).

Another polarization technique use for the effect of Love (SH) wave effect minimization for a single 3 component sensor recording is term as RayDec technique (Hobiger et.al, 2009) The vertical component is taken as master trigger as because the SV arrival occur only on the vertical component, while stacking a large number of horizontal component to obtained ellipticity of Rayleigh curve (Hobiger et al., 2009) showed that the obtained ellipticity will be closer to the true ellipticity curve rather than the H/V curve.

To elaborate RayDec techniques consider a signal {where $x(t) = e(t)$ or $n(t)$ or $v(t)$ }. These three time series has N number of data points and having length T. To obtain a Rayleigh wave ellipticity curve, the main idea of this method is to obtain only Rayleigh waves in comparison with other waves type by the addition of a large number of filtered signal windows Δ, estimates the energy level of horizontal averaged and vertical signal in a location where the vertical component change its sign from -ve to +ve. Due to the phase shift of $\frac{\pi}{2}$ between Rayleigh wave vertical and horizontal component, both the horizontal component of EW and NS are projected by factor ϕ with north direction in such a way to maximized the correlation between the summed horizontal and vertical component. The Rayleigh wave ellipticity is obtained latterly from Eq.5 . The ellipticity E is calculated as the square root of the ratio of the energies in the signal window. Δ.

$$\mathbf{E} = \sqrt{\frac{\int_0^{\Delta} \mathbf{hf^2.s(t)*dt},}{\int_0^{\Delta} \mathbf{vf^2.s(t)*dt}}} \qquad (5)$$

where hf.s (t) is the horizontal average (NS north-south , EW east-west) signal and Vf.s (t) is the vertical component. This process is repeated for a whole record for an increment of window length Δ .The window length is taken as function of frequency such that to ensure 10 significant cycle at chosen frequency (Δ=10/f where f is the analyzing frequency from 0.2 to 20 Hz are used). There are two tuning parameters for this technique , Δ (window length) and df (width of frequency filter). The effect of these two tuning parameter on the result is shown Fig.8. For our analysis we used one-hour records of noise, which were divided into 6 segments of 10 minutes each , afterward, the result is average out for all the six segments with the aim of minimization of

misfit (see for detail procedure Hobiger et al., 2009). The result of ellipticity obtained via RayDec show a better match with borehole curve especially at right and left limb.

The analysis of both time-frequency and RayDec for H/V give satisfactory result for the ellipticity retrieval of Rayleigh waves. Fig 9 shows the comparison of all the technique retrieved curves with that of borehole ellipticity.

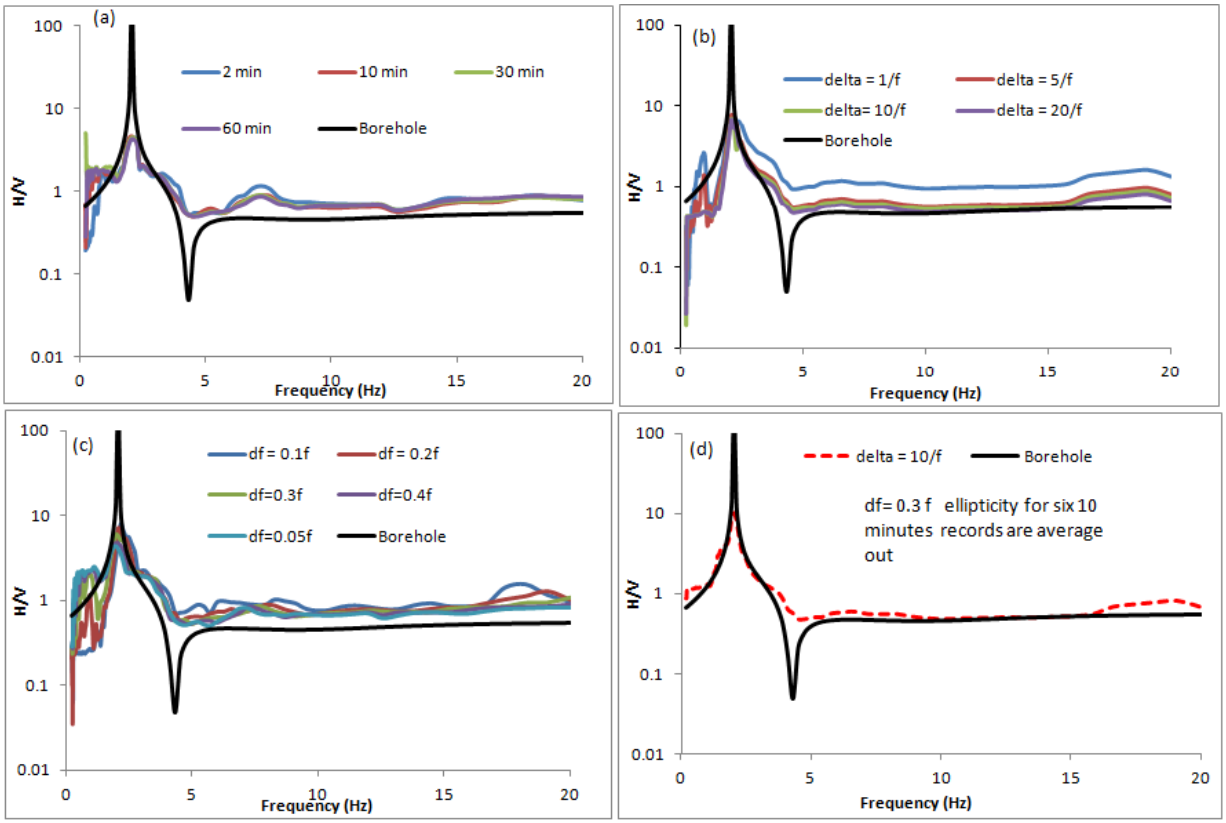

Fig.8 Ellipticity obtained via RayDec technique , (a) shows the effect signal duration on the result.(b) shows the effect of using different width of window (c) shows the effect of different filter width on the result (d) shows six 10-minute windows (ellipticity for each 10 minute is obtained at the end the result is average and compared with borehole data black line).

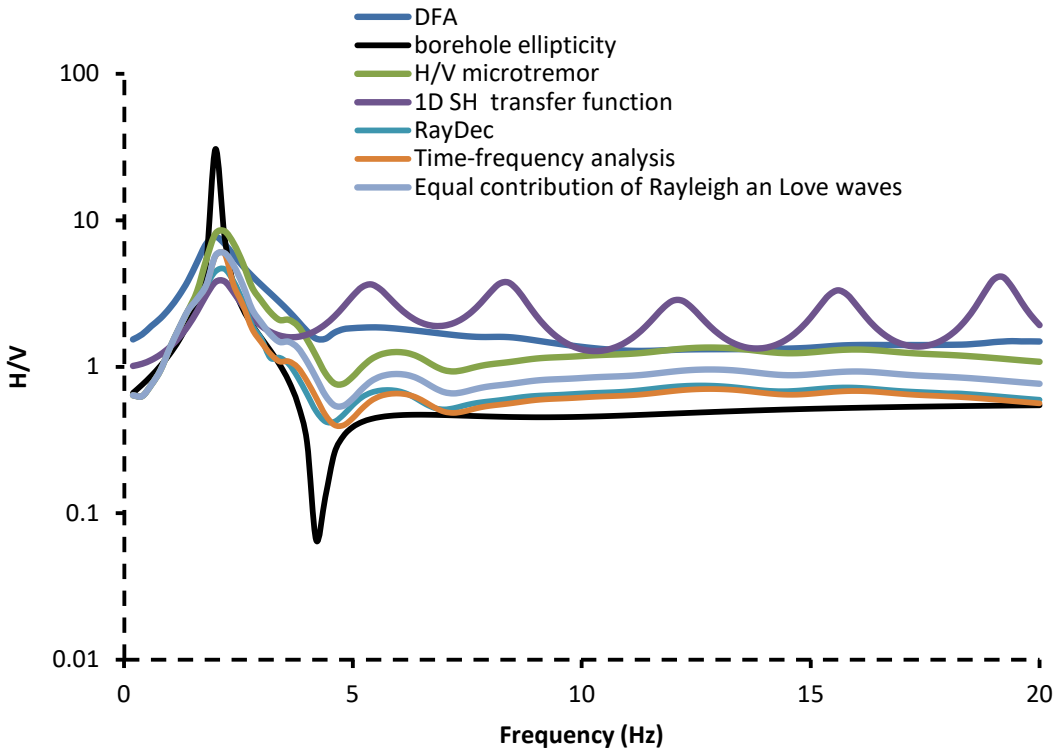

Fig.9Show the comparison of borehole ellipticity curve combine with that of all elliptcity retrieval technique.

7.Joint inversion of the ellipticity and dispersion curve.

The ellipticity curve retrieved from both the time-frequency analysis and RayDec technique are jointly inverted along with theoretical dispersion curve of the borehole obtained by forward modeling (using code gpdc, http://www.geopsy.org last accessed 1-29-2017). The frequency range of the dispersion curve is considered above the fundamental frequency of the site 2Hz (in our case) till 45 Hz, below the fundamental frequency of the site dispersion curve is difficult to retrieved for Rayleigh waves ,as the medium filter out all the lower frequencies (Scherbaum et al, 2003). To get the 1D shear wave velocity from dispersion and these H/V curve, the modified neighborhood algorithm (NA) proposed by Wathelet (2008) are used. In comparison to linearized inversion procedure, NA is a derivative-free procedure. NA is considered very good inversion strategy because it has the advantage over the other approaches as it utilizes all previous model information to sample the new model (Sambridge 1999). The parameters for inversion are considered as follow: the numbers of layers are considered to be four above the bedrock, P-wave velocity are linked with S-wave velocity, S-wave velocity are allowed to linearly increased from surface to the bedrock, density is taken constant at 2000 kg/m3, while the Poisson ratio are considered to change from 0.2 to 0.5. The inversion is made for time-frequency and RayDec based H/V curve only, as that of DFA H/V curve contains the effect of all wave-type and its inversion with Rayleigh wave dispersion curve will certainly give bias result. The misfit between all generated models and target curves (dispersion and H/V) are calculated using eq. 6.

$$misfit = \frac{1}{N}\sqrt{\sum((x_t(f) + x_m(f))^2 / x_t(f)^2)} \quad (6)$$

where $x_t(f)$ is the target curve (either experimental H/V or borehole dispersion curve) at frequency (*f*) while $x_m(f)$ is the modeled curve for both H/V and dispersion curve, N is the number of points of target curve considered for inversion. The misfit for both the target (dispersion and H/V) are weighted average. Hobiger et al (2013) analyzed that which part of ellipticity is carrying the most important information about the surface structure. He concluded that right limb up to the trough is the most responsive part of curve to the subsurface target. However to constraint the peak of the H/V curve (which is carrying important information about the depth of bedrock) we have considered the left limb of the H/V curve as well for the inversion , therefore the frequency range of the H/V considered from 1 to 4.2Hz. The result of the inversion are shown in Fig.10. The results shows that in both the cases (Time-frequency analysis and RayDec based H/V curves),the best fit inverted model is very near to original borehole model.

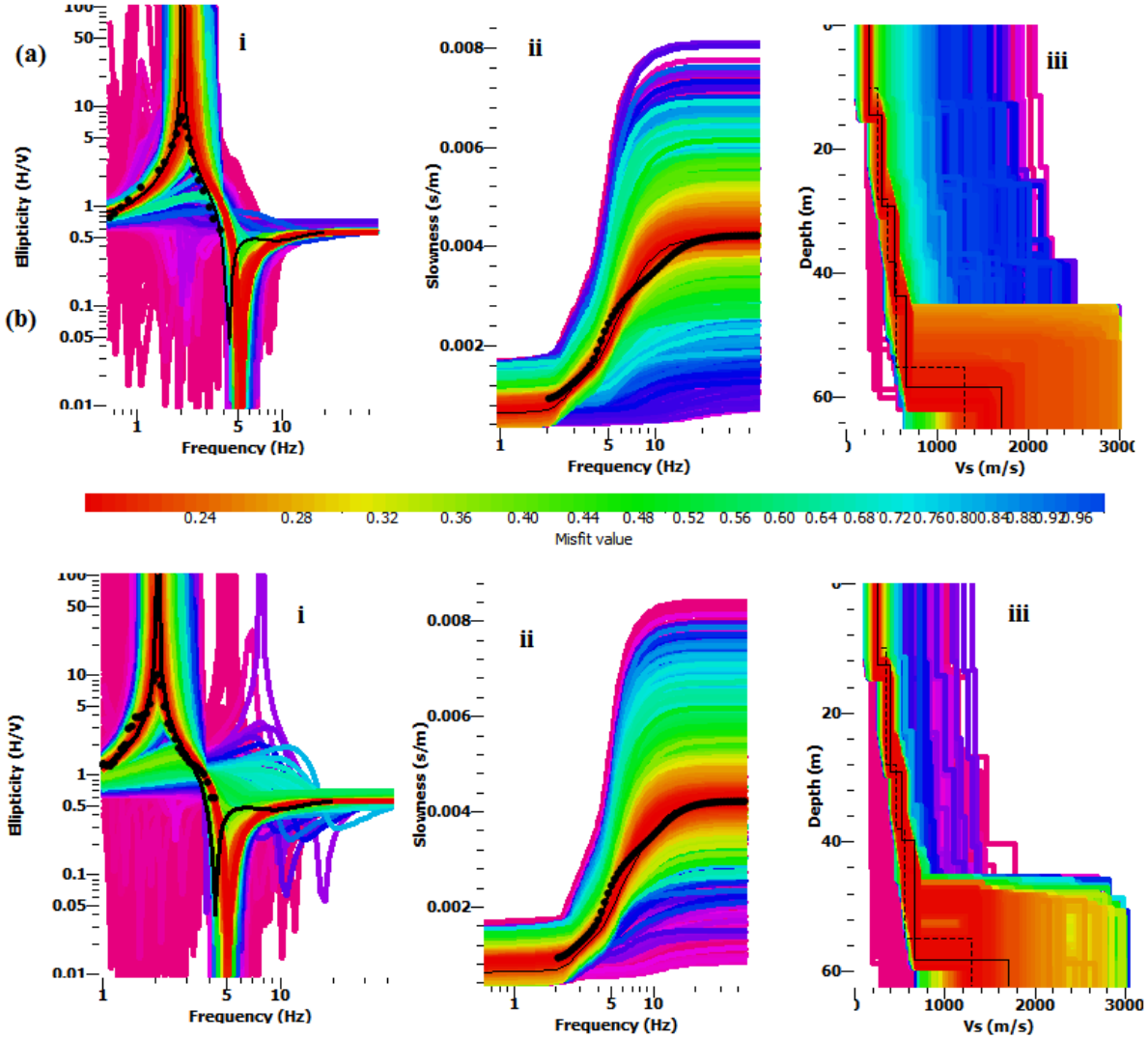

Fig.10 Shows the inversion result of time-frequency Fig.10(a,i) RayDec H/V curve Fig.10(b,i) along with the borehole dispersion curve. Dotted line in both cases (10ab,i,ii) indicate the target curve while soild line show the best fit model response (10ab,i,ii).In Fig.10ab.iii, all the inverted models are shown dashed line borehole model while solid line the bestfit model.

7.Discussion and conclusion.

Deep soil shear wave velocity information can be retrieved from the joint inversion of H/V curve with dispersion curve. The H/V curve is assumed to be linked with Rayleigh wave ellipticity for a site. However in real situation the H/V curve technique can not completely replicate the Rayleigh wave ellipticity. It is because of the presence of different elastic wave influence presence in the H/V curve retrieval. Diffuse field approach is a better way to consider the effect of all elastic seismic phases (body and surface wave). However the analysis of our data shows that at singularities (peak and trough) especially at peak of the H/V curve obtained via DFA is very well correlated with Rayleigh ellipticity curve in term of these singularities frequency. This matching can be assumed that around the peak frequency even in case of diffuse like field situation the seismic noise field is dominated by surface wave especially Rayleigh waves.

The other approach used for the H/V curve technique is linked to the surface wave dominancy especially Rayleigh wave around the singularities. Three different polarization technique for retrieval of ellipticity curve by minimizing the SH contribution to the horizontal component is comparable to H/V curve with equal contribution of Rayleigh and Love wave, time-frequency analysis and RayDec technique. The result of equal assumption of Rayleigh/Love wave fraction is unable to match with parts of borehole ellipticity except at peak. However ellipticity curve retrieved from noise analysis through time-frequency and RayDec shows a good replication of borehole ellipticity around the peak, right and left limb.

For the deep soil deposit the joint inversion of ellipticity and dispersion curve of Rayleigh wave are recommended. However due to the presence of effect of other seismic elastic phases especially Love wave may produced some bias result. Therefore it is extremely necessary to retrieved a H/V curve where the effect of Love wave contribution are minimized prior to the inversion with dispersion curve. For our test site we found that time-frequency and RayDec show better result Fig.10,by replication left and right limb of ellipticity curve of the borehole at the study.

Acknowledgement.

We are thankful to the Sanchez-Sesma (Instituto de Ingeniería Universidad Nacional Autónoma de México) for sharing his code for DFA analysis of seismic noise. We appreciate the help from of Hobiger (ETH Zurich) and Marc Wathelet (University Joseph Fourier - Grenoble 1, Grenoble) . We are indebted to Marcelo Assumpcao, Galiardo , Felipe Neves (Instituto de Astronomia, Geofísica e Ciências Atmosféricas, university of Sao Paulo) for providing the instruments for recoding and technical assistance. This work is completed with help of TWAS-CNPq for

fellowship grant number 190038/2012-8 (CNPq/TWAS - Full-Time Ph.D. Fellowship - GD 2012) for financial support.

References:

[1]. Aki, K., and P.G. Richards Quantitative seismology, Second Edition, University Science Books.**2002**

[2]. Arai, H., and K. Tokimatsu. Evaluation of local site effects based on microtremor H/V spectra. Proceeding of the Second International Symposium on he Effects of Surface Geology on Seismic Motion. Yokohama, Japan. **,1998,2** 673-680.

[3]. Bard, P.Y.: Microtremor measurements: a tool for site effect estimation?. The Effects of Surface Geology on Seismic Motion, eds. K. Irikura, K. Kudo, H. Okada and T. Sasatani (Balkema, Rotterdam), **1999,** 1251-1279.

[4]. Bonnefoy-Claudet, S., Cornou, C.,Bard, P.-Y., Cotton, F.,Moczo, P., Kristek, J. & F¨ah, D., 2006a. H/V ratio: a tool for site effects evaluation. Results from 1-D noise simulations, *Geophys. J. Int.*, **2006;** 827–837.

[5]. Bormann, P. (2002). NMSOP – New Manual of Seismological Observatory Practice. IASPEI. GeoForschungsZentrum Potsdam, Germany. **2002.**

[6]. Chouet, B., De Luca, G., Milana, G., Dawson, P., Martini, M., Scarpa, R.. Shallow velocity of Stromboli volcano, Italy, derived from small-aperture array measurements of Strombolian tremor. Bull. Seism. Soc. Am.,**1998,** 88-3, 653-666.

[7]. Cornou, C. Traitement d'antenne et imagerie sismique dans l'agglomération grenobloise (Alpes françaises): implications pour les effets de site (In french). Université Joseph Fourier, **2002,**260.

[8]. D. Fäh, M . Wathelet, M. Kristekova, H. Havenith, B. Endrun, G. Stamm, V. Poggi, J. Burjanek, and C. Cornou. Using ellipticity information for site characterisation. NERIES deliverable JRA4 D4.**2009** [Online]. Available: http://www.neries-eu.org

[9]. Endrun, B. Love wave contribution to the ambient vibration H/V amplitude peak observed with array measurements, J. Seismol., **2011 15,** 443–472.

[10]. Hobiger, M., P.-Y. Bard, C. Cornou, and N. Le Bihan (2009), Single station determination of Rayleigh wave ellipticity by using the random decrement technique (RayDec), Geophys. Res. Lett., 36, L14303, doi:10.1029/2009GL038863.

[11]. Horike, M. Inversion of phase velocity of long period microtremors to the S-wave-velocity structure down to the basement in urbanized areas. J. Phys. Earth, **1985**. 33, 59-96.

[12]. Kohler, A., Ohrnberger, M. & Scherbaum, F., (2006). The relative fraction of Rayleigh and Love waves in ambient vibration wavefields at different European sites, in *Proceedings of the 3rd Int. Symp. on the Effects of Surface Geology on SeismicMotion*, Grenoble, 30 August–01 September,Vol. 1, pp. 351–360

[13]. Konno, K., and T. Ohmachi .Ground-Motion Characteristic Estimated from Spectral Ratio between Horizontal and Vertical Components of Microtremor. Bull. Seism. Soc. Am., **1998**. 88, 228-241.

[14]. Li, T. M. C., Ferguson, J. F., Herrin, E., D. H. B. High-frequency seismic noise at Lajitas, Texas. Bull. Seism. Soc. Am., **1984**., **74-5**, 2015-2033.

[15]. Lunedei and Malischewsky 2015 . A Review and Some New Issues on the Theory of the H/V Technique for Ambient Vibrations , Perspectives on European Earthquake Engineering and Seismology, Geotechnical, Geological and Earthquake Engineering 371-390,DOI 10.1007/978-3-319-16964-4_15.

[16]. M. Hobiger,, C. Cornou,1 M. Wathelet,G. Di Giulio,B. Knapmeyer Endrun, F. Renalier,P.-Y. Bard,1 A. Savvaidis, S. Hailemikael,N. Le Bihan,M. Ohrnberger and N. Theodoulidis Ground

structure imaging by inversions of Rayleigh wave ellipticity sensitivity analysis and application to European strong-motion sites Geophys. J. Int. **2013 192,** 207–229.

[17]. Mucciarelli M. and Gallipoli M.R.; 2001: *A critical review of 10 years of microtremor HVSR technique.* Boll. Geof.Teor. Appl. **2001**, **42**, 255-266.

[18]. Mulargia, F., 2012. The seismic noise wave field is not diffuse, J. acoust. Soc. Am., 131, 2853.

[19]. Okada, H. The Microtremor Survey Method. Geophys. Monograph Series, **2003** SEG, 129 pp

[20]. Perton, M., S´anchez-Sesma, F.J., Rodr´ıguez-Castellanos, A., Campillo, M. & Weaver, R.L.. Two perspectives on equipartition in diffuse elastic fields in three dimensions, *J. acoust. Soc. Am.*, **2009**, **126**(3), 1125–1130.

[21]. Picozzi, M., Parolai, S., Richwalski, S.M. Joint inversion of H/V ratios and dispersion curves from seismic noise: Estimating the S-wave velocity of bedrock. Geoph. Res. Lett., 32, No.11, **2005** doi: 10.1029/2005GL022878

[22]. Piña-Flores J., Perton M., García-Jerez A., Carmona E., Luzón F., Molina-Villegas J.C., Sánchez-Sesma F.J. (2017). The inversion of spectral ratio H/V in a layered system using the Diffuse Field Assumption (DFA), Geophysical Journal International, In press.

[23]. Porsani , Welitom Borges, Vagner Roberto Elis , Liliana Alcazar Diogo .Investigações geofísicas de superfície e de poço no sítio controlado de geofísica rasa do IAGUSP, Revista Brasileira de Geofísica.**2004**.

[24]. Sambridge, M. (1999). Geophysical inversion with a Neighbourhood algorithm, I, Searching a parameter space. Geophys. J. Int., 138, 479–494

[25]. Sanchez-Sesma, F.J. *et al.*,. A theory for microtremor H/V spectral ratio: application for a layered medium, *Geophys. J. Int.*, **2011**, **186**(1), 221–225.

[26]. Scherbaum, F., K.-G. Hinzen, and M. Ohrnberger,. Determination of shallow shear-wave velocity profiles in Cologne, Germany area using ambient vibrations. Geophys. J. Int.**2003**, 152, 597-612.

[27]. SESAME scientific products(2001-2004) http://SESAME.geopsy.org/SES_Reports.htm

[28]. Tokimatsu, K. (1997). Geotechnical site characterization using surface waves. Earthquake Geotechnical Engineering, Ishihara (ed.), Balkema, Rotterdam, 1333-1368.

[29]. Wathelet, M., (2008). An improved neighborhood algorithm: parameter conditions and dynamic scaling, Geophys. Res. Lett., **35,** L09301,doi:10.1029/2008GL033256.

[30]. Yamamoto, H. (2000). Estimation of shallow S-wave velocity structures from phase velocities of love- and Rayleigh- waves in microtremors. Proceedings of the 12th World Conference on Earthquake Engineering. Auckland, New Zealand, **2000.**

[31]. Yamanaka, H., Takemura, M., Ishida, H, Niwa, M. Characteristics of long-period microtremors and their applicability in exploration of deep sedimentary layers. Bull. Seism. Soc. Am. **1994**., 84, 1831-1841.A.